

1 **Best practices for precipitation sample storage for offline studies of ice nucleation in marine and coastal environments**

2 Charlotte M. Beall<sup>1</sup>, Dolan Lucero<sup>2</sup>, Thomas C. Hill<sup>3</sup>, Paul J. DeMott<sup>3</sup>, M. Dale Stokes<sup>1</sup>, Kimberly A. Prather<sup>1,4</sup>

3 <sup>1</sup>Scripps Institution of Oceanography, University of California San Diego, La Jolla, CA, 92037, USA

4 <sup>2</sup>Department of Earth and Environmental Science, New Mexico Institute of Mining and Technology, Socorro, NM, 87801,  
5 USA

6 <sup>3</sup>Department of Atmospheric Sciences, Colorado State University, Fort Collins, CO, 80523, USA

7 <sup>4</sup>Department of Chemistry and Biochemistry, University of California San Diego, La Jolla, CA, 92093, USA

8

9 *Correspondence to:* Kimberly A. Prather (kprather@ucsd.edu)

10 **Abstract.** Ice nucleating particles (INPs) are efficiently removed from clouds through precipitation, a convenience of nature  
11 for the study of these very rare particles that influence multiple climate-relevant cloud properties including ice crystal  
12 concentrations, size distributions, and phase-partitioning processes. INPs suspended in precipitation can be used to estimate  
13 in-cloud INP concentrations and to infer their original composition. Offline droplet assays are commonly used to measure INP  
14 concentrations in precipitation samples. Heat and filtration “treatments” are also used to probe INP composition and size  
15 ranges. Many previous studies report storing samples prior to INP analyses, but little is known about the effects of storage on  
16 INP concentration or their sensitivity to treatments. Here, through a study of 15 precipitation samples collected at a coastal  
17 location in La Jolla, CA, USA, we found INP concentration changes up to > 1 order of magnitude caused by storage to  
18 concentrations of INPs with warm to moderate freezing temperatures (-7 to -19 °C). We compared four conditions: 1.) storage  
19 at room temperature (+21-23 °C), 2.) storage at +4 °C 3.) storage at -20 °C, and 4.) flash freezing samples with liquid nitrogen  
20 prior to storage at -20 °C. Results demonstrate that storage can lead to both enhancements and losses of greater than one order  
21 of magnitude, with non-heat-labile INPs being generally less sensitive to storage regime, but significant losses of INPs smaller  
22 than 0.45 µm in all tested storage protocols. Correlations between total storage time (1-166 days) and changes in INP  
23 concentrations were weak across sampling protocols, with the exception of INPs with freezing temperatures  $\geq$  -9 °C in  
24 samples stored at room temperature. We provide the following recommendations for preservation of precipitation samples  
25 from coastal or marine environments intended for INP analysis: that samples be stored at -20 °C to minimize storage artifacts,  
26 that changes due to storage are likely an additional uncertainty in INP concentrations, and that filtration treatments be applied  
27 only to fresh samples. At the freezing temperature -11 °C, average INP concentration losses of 51%, 74%, 16% and 41% were  
28 observed for untreated samples stored using the room temperature, +4 °C, -20 °C, and flash frozen protocols, respectively.  
29 Finally, the estimated uncertainties associated with the 4 storage protocols are provided for untreated, heat-treated and filtered  
30 samples for INPs between -9 and -17 °C.

31

32 **1. Introduction**

33 In-cloud ice crystals and their formation processes are critical features of Earth's radiative and hydrological balance, affecting  
34 multiple climate-relevant cloud properties including cloud lifetime, reflectivity, and precipitation efficiency (DeMott et al.,  
35 2010; Lohmann, 2002; Lohmann and Feichter, 2005; Tan et al., 2016; Creamean et al., 2013). Ice nucleating particles (INPs)  
36 impact ice crystal concentrations and size distributions in clouds by triggering the freezing of droplets at temperatures above  
37 the homogeneous freezing point of water ( -38 °C).

38 INPs have been sampled in clouds and precipitation for decades (e.g. Rogers et al., 1998; Vali, 1971; Vali, 1966) to measure  
39 abundances, probe their compositions and investigate the extent to which they impact the properties of clouds. There are  
40 several caveats to consider when inferring in-cloud INP concentrations or properties from precipitation samples (Petters and  
41 Wright, 2015), including “sweep-out” of additional INPs as the hydrometeor traverses the atmosphere below the cloud (Vali,  
42 1974) and heterogeneous chemistry due to adsorption or absorption of gases (Hegg and Hobbs, 1982; Kulmala et al., 1997;  
43 Lim et al., 2010). However, assessing the composition of INPs in precipitation samples is more straightforward than cloud  
44 particles. Thus, the number of publications reporting measurements of INP concentrations in precipitation has increased over  
45 the past decade. Numerable insights have been obtained in previous precipitated-based INP studies, including the efficient  
46 depletion of INPs relative to other aerosols of similar size in precipitating clouds (Stopelli et al., 2015), constraints on minimum  
47 enhancement factors for secondary ice formation processes (Petters and Wright, 2015), and the identification, characteristics  
48 and distribution of various INP populations (e.g. Christner et al., 2008a; Hader et al., 2014; Stopelli et al., 2017). INP  
49 concentrations in precipitation have been used to estimate in-cloud concentrations, based on assumptions that the majority of  
50 particles (86%) in precipitation originate from the cloud rather than the atmospheric column through which the hydrometeor  
51 descended (Wright et al., 2014). Along the same line of reasoning, INPs in precipitation have also been used to infer sources  
52 and composition of in-cloud INP populations (e.g. Martin et al., 2019 and Michaud et al., 2014, respectively).

53 A number of online (real-time) and offline (processed post-collection) techniques exist for measurement of INPs for each ice  
54 nucleation mechanism, including condensation, deposition, immersion and contact freezing. However, as some simulations  
55 have shown that immersion mode freezing is the dominant mode of primary freezing in the atmosphere between 1000 and  
56 200 hPa (Hoose et al, 2010), most techniques target immersion freezing. Despite the lack of time resolution, offline  
57 techniques enable measurement of INPs at modest supercooling (e.g. up to -5 °C) and temperature regimes where  
58 concentrations typically fall below detection limits of online instruments (DeMott et al., 2017). Offline instruments capable  
59 of immersion mode INP measurement include a number of droplet assays, in which sample suspensions are distributed  
60 among an array of droplets that are then cooled and frozen (e.g. Budke and Koop, 2015, Harrison et al., 2018, Hill et al.,  
61 2014, Whale et al., 2015) as well as other systems in which water is condensed onto particles collected on substrates prior to  
62 cooling and freezing (e.g. Mason et al., 2015). As they are designed for analysis of liquid suspensions, droplet freezing  
63 assay techniques are commonly used for measurement of INPs suspended in precipitation (e.g. Creamean et al., 2019,  
64 Rangel-Alvarado et al., 2015, Michaud et al., 2015, Stopelli et al., 2014, Wright et al., 2014).

65 Many studies report results from samples stored prior to processing. Storage protocols vary widely, including total storage  
66 time, time between collection and storage, and temperature fluctuations between collection, shipment and storage (if these  
67 details are provided at all, see summary Table S1). Storage temperatures range from -80 °C (Vali et al., 1971) to +4 °C (e.g.  
68 Petters and Wright, 2015, Failor et al., 2017, Joyce et al., 2019), yet generally samples are stored between +4 °C and -20 °C.  
69 Reported storage intervals range between hours (Schnell et al., 1977; Christner et al., 2008) to 48 years (Vasebi et al., 2019).  
70 The understanding of storage effects on INPs suspended in precipitation is limited (Petters and Wright, 2015), and the  
71 understanding of storage effects on INPs collected on filters is similarly lacking (Wex et al., 2019). Stopelli et al. (2014a)  
72 studied INP concentrations in a snow sample stored at +4 °C and observed a decrease in the concentration of INPs active at -  
73 10 °C over 30 days by a factor of ~2. Schnell (1977) reported significant losses in fog and seawater samples after storage at  
74 room temperature for short periods (6-11 hours). Several studies have reported on the lability of commercially available dust  
75 and biological IN entities in storage above 0 °C or under freezing conditions, including Arizona Test Dust and SnoMax®  
76 (Perkins et al., 2020; Polen et al., 2016; Wex et al., 2015), and similar labilities could affect the INPs of similar composition  
77 in precipitation samples (Creamean et al., 2013; Martin et al., 2019). Considering the abundance of precipitation based INP  
78 studies, the lack of bounds on potential impacts of storage on INP concentration measurements represents a critical  
79 uncertainty in conclusions derived from data on stored samples. Furthermore, to determine INP activation mechanisms and  
80 composition, previous studies have applied “treatments” to precipitation samples, including heat, filtration, enzymes and  
81 peroxide, (e.g. Hill et al., 2014) but it is unknown to what extent storage affects the results of such experiments.

82 Here we investigate the effects of four storage protocols on INPs using 15 precipitation samples collected between 9/22/2016  
83 and 11/22/2019 at two coastal sites at Scripps Institution of Oceanography, La Jolla, CA, USA: 1.) storage at room temperature  
84 (+ 21-23 °C) , 2.) storage at +4 °C (“refrigerated”), 3.) storage at -20 °C (“frozen”), and 4.) flash freezing samples with liquid  
85 nitrogen prior to storage at -20 °C (“flash frozen”). The abundance of previous studies that report storage between +4 °C and  
86 -20 °C motivated the choice of techniques 2 and 3 (see Table S1). Room temperature storage was chosen to provide context  
87 as a “worst-case scenario”, and the flash freezing technique was chosen to investigate whether any changes of INP  
88 concentrations could be mitigated by instantaneous freezing prior to storage. The 15 precipitation samples in this study were  
89 divided into several replicates so that the concentration of INPs could be measured in untreated, heated, and filtered samples  
90 when fresh, and again after storage using the 4 techniques described above. Sample replicates were additionally processed at  
91 2 different points in time to investigate the effects of total storage time on INP concentration measurements. Enhancements  
92 and losses of INPs according to storage protocol and treatment are reported, as well as recommendations for storage protocols  
93 that best preserve INPs in untreated, heated, and filtered precipitation samples from marine or coastal environments.

## 94 **2. Methods**

### 95 **2.1 Precipitation Sample Collection**

96 Precipitation samples were collected at two coastal locations at Scripps Institution of Oceanography (32.87 N 177.25 W): the  
97 rooftop of the Ellen Browning Scripps Memorial Pier laboratory (32.8662 °N, 117.2544 °W) (10 meters above sea level) and

98 the rooftop of a storage container next to Isaacs Hall (32.8698 °N, 117.2522 °W, 58 meters above sea level, 500 m inland).  
99 Collection technique varied based on location. At the SIO pier, the Teledyne ISCO model 6712 commercial water sampler  
100 (Teledyne ISCO, Inc., US) was used. A plastic funnel, 27 cm in diameter, and Tygon tubing, connected the sampler inlet to  
101 the water sampler's distributor arm. The samples were distributed via the distributor arm into one of twenty-four 1-liter  
102 polypropylene bottles on an hourly time interval. Bottles corresponding to consecutive 1-hour time intervals were combined  
103 when the hourly precipitation volume was insufficient for sample separation and analysis (< 50 mL per bottle). At the Isaacs  
104 Hall location, an ISO 6706 plastic graduated cylinder and plastic funnel, 27 cm in diameter, was used for precipitation  
105 collection. At both sites, ring stands supported the collection funnels approximately 60 cm above the rooftop. All funnels,  
106 tubing, cylinders, and bottles were cleaned with 10% hydrogen peroxide for 10 minutes and rinsed with milli-Q purified water  
107 three times immediately before each sampling event. Satellite composites from the National Weather Service Weather  
108 Prediction Center's North American Surface Analysis Products were used for synoptic weather analysis to generally  
109 characterize each rain event (see Table 1). Atmospheric river (AR) events were identified using the AR Reanalysis Database  
110 described in (Guan and Waliser, 2015) and (Guan et al., 2018).

## 111 **2.2 Storage Protocols**

112 The following sample storage protocols were used: frozen at -20 °C, refrigerated at 4 °C, room temperature (21 - 23 °C), and  
113 flash freezing, or flashing with liquid nitrogen (-196 °C) before frozen at -20 °C. All techniques except storage at room  
114 temperature are commonly used for offline INP analysis (see Table S1). Excluding the samples that were flash frozen, all  
115 samples were stored in 50 mL sterile plastic Falcon® tubes (Corning Life Sciences, Corning, NY, USA). Flash frozen samples  
116 were stored in polypropylene 5 mL cryovials. Prior to storage, 25 - 50 mL bulk sample aliquots were distributed from collection  
117 bottles into Falcon® tubes, shaking bottles ~10 s between each distribution. Not all samples were stored using all four of the  
118 storage protocols due to limited volume for some samples. See Tables 2-4 for a summary of the number of samples studied for  
119 each storage protocol. Precipitation samples were stored for varying intervals between 1 and 166 days to investigate effects of  
120 storage time on INP concentrations. INP measurements were made in two or three time steps: within two hours of collection,  
121 and once or twice after storing using one of four storage protocols described above, depending on volume. Stored and fresh  
122 samples were analysed in three treatment conditions: 1) raw untreated precipitation, 2) heated over a 95 °C water bath for 20  
123 minutes and 3) filtered through a 0.45 µm surfactant-free cellulose acetate syringe-filter (Thermo Scientific™ Nalgene™,  
124 Waltham, MA, USA). Heat treatments and filters were applied to samples just prior to processing (i.e. treatments were not  
125 applied to samples prior to storage).

## 126 **2.3 INP Analysis**

127 The automated ice spectrometer (AIS) is an offline immersion-mode freezing assay which is described elsewhere (Beall et al.,  
128 2017). Briefly, 50 µL aliquots of sample are pipetted into two sterile 96-well polypropylene PCR plates. The plates are inserted  
129 into an aluminium block, machined to hold PCR plates, that sits in the coolant bath of a Fisher Scientific Isotemp® Circulator.  
130 A thermistor placed atop the left side of the aluminium block, below the PCR plate, recorded temperature. An acrylic plate  
131 separated the PCR plates from the ambient lab air. In the headspace between the acrylic plate and the PCR plates, nitrogen gas

132 flowed at a flow rate of 14 Lpm to reduce temperature stratification in the samples (Beall et al., 2017). The nitrogen gas was  
133 cooled before emission by passing through the chiller via copper tubing. A 0.5 Megapixel monochrome camera (Point Grey  
134 Blackfly 0.5MP Mono GigE POE) performed the image capture. Custom LabView software controlled the camera settings,  
135 the rate the chiller cooled, and displayed the temperature of the thermistor.

136 A control milli-Q water sample is used, typically in the first 30 wells of each sample run, to detect contamination and for  
137 subsequent INP concentration calculations. Thirty wells were used per sample to achieve a limit of detection of 0.678 IN mL  
138  $^{-1}$ . For each run, the chiller was cooled to -35°C. As the chiller cools the sample plates (1 °C/min), the custom LabView virtual  
139 instrument records the location and temperature of the freezing event as they occur. Freezing events are detected by the change  
140 in pixel intensity of the sample as it changes from liquid to solid.

#### 141 **2.4 Particle Size Distributions**

142 Size distributions of insoluble particles suspended in the fresh and stored precipitation samples were measured using the Multi-  
143 sizing Advanced Nanoparticle Tracking Analysis (MANTA) ViewSizer 3000 (Manta Instruments Inc.). The Manta ViewSizer  
144 3000 applies multi-spectral particle tracking analysis (m-PTA) to obtain size distributions of particles of sizes between 10 and  
145 2000 nm with three solid-state lasers with wavelengths of 450 nm, 520 nm and 650 nm. m-PTA has been shown to outperform  
146 traditional dynamic light scattering (DLS) techniques when measuring polydisperse particles in suspension (McElfresh et al.,  
147 2018). For analysis, 300 videos of the illuminated particles in suspension are recorded, each 10 seconds in length. The software  
148 tracks each particle individually, obtaining particle size and number concentration from their Brownian motion and the imaged  
149 sample volume.

150

### 151 **3 Results**

#### 152 **3.1 INP concentrations in fresh precipitation samples**

153 Figure 1 shows INP concentrations of 15 coastal rain samples, collected in a variety of meteorological conditions including  
154 scattered, low coastal rainclouds, frontal rain, and atmospheric river events (see Table 1). Observations generally fall within  
155 bounds of previously reported INP concentrations from precipitation and cloud water samples (grey shaded region, adapted  
156 from Petters and Wright, 2015). Observed freezing temperatures ranged from -4.0 to -18.4 °C, with concentrations up to the  
157 limit of testing at  $10^5$  INP L $^{-1}$  precipitation. AIS measurement uncertainties are represented with 95% binomial sampling  
158 intervals (Agresti and Coull, 1998).

159 Following the assumptions in (Wright and Petters, 2015) to estimate in-cloud INP concentrations from precipitation samples  
160 (i.e. condensed water content of 0.4 g m $^{-3}$  air), observations of INP concentrations in fresh precipitation samples are  
161 additionally compared to studies of field measurements conducted in marine and coastal environments. Figure 1 shows that  
162 atmospheric INP concentration estimates compare with INP concentrations observed in a range of marine and coastal  
163 environments, including the Caribbean, East Pacific, and Bering Sea, as well as laboratory-generated nascent sea spray aerosol  
164 (DeMott et al., 2016). However, two of the warmest-freezing INP observations in Fig. 1 (at -4.0 and -4.75 °C) exceed  
165 temperatures commonly observed in marine-influenced atmospheres, precipitation and cloudwater samples.

166 In 5 of the 15 heat-treated samples, INP concentrations were increased by 1.9 – 13X between -9 and -11 °C (see Discussion).  
167 Excluding these 5 samples, the fraction of heat-resilient INPs varied between samples and generally increased with decreasing  
168 temperature. Geometric means and standard deviations of heat-treated:untreated INP ratios were  $0.40 \times/\div 1.9$ ,  $0.51 \times/\div 2.0$ ,  
169 and  $0.62 \times/\div 2.1$  at -11, -13, and -15 °C respectively.

170 Fractions of INPs  $< 0.45 \mu\text{m}$  also varied between samples, with geometric means and standard deviations of  $0.48 \times/\div 1.73$ ,  
171  $0.30 \times/\div 3.4$  and  $0.37 \times/\div 1.9$  at -11, -13, and -15 °C respectively. Mean values of heat-resilient INP fractions and INPs  $< 0.45$   
172  $\mu\text{m}$  were calculated using the geometric mean, which is more appropriate than the arithmetic mean for describing a distribution  
173 of ratios (Fleming and Wallace, 1986).

### 174 **3.2 Effects of sample storage on INP concentration measurements**

175 INP concentrations of stored replicate samples are compared with original fresh precipitation samples in Figures 2-4, calculated  
176 in successive 2 °C increments between -7 and -19 °C. This temperature range was chosen for the analysis because most fresh  
177 precipitation samples exhibited freezing activity between -7 and -19 °C. Numbers of datapoints in Figs 2-4 differ across the  
178 temperature intervals due to limits of detection (i.e. ratios were not calculated at temperatures where zero or all wells were  
179 frozen in the fresh and/or stored sample).

180 All stored:fresh ratios were calculated from cumulative INP distributions in 2 °C intervals, meaning that the INP concentration  
181 in each interval is inclusive of the concentration in all of the preceding (warmer) temperature intervals. The choice of the  
182 cumulative distribution was motivated by the fact that it is standard in INP studies to report INP concentrations in terms of the  
183 cumulative distribution, and it is important to consider impacts of storage on cumulative INP distributions and any conclusions  
184 derived from them. Thus, in this study, deviations observed in a stored sample are not necessarily independent, i.e. the  
185 sensitivity of INPs to storage in one temperature interval could impact the observed changes in all of the following (colder)  
186 temperature interval. For example, in fresh untreated precipitation samples (see Fig. 1), 32% of the INP concentration  
187 calculated at -11 °C activated in one of the preceding (warmer) 2 °C temperature intervals. At -17 °C, this fraction is increased  
188 to 46%.

189 To investigate correlations between sample storage time and INP enhancements or losses, duplicate samples were archived  
190 (when sufficient volume was available) so that each sample could be processed at two distinct points post-collection (see  
191 example Fig. S1). For INPs with freezing temperatures  $\geq -9$  °C in samples stored at room temperature, time is moderately  
192 correlated with changes in INP concentrations ( $R^2 = 0.58$ ). Figure S5 shows how losses of warm-freezing INPs in samples  
193 stored at +4 °C and room temperature impact the cumulative INP spectra for a select sample. Beyond these exceptions, little  
194 to no correlation between storage time and INP enhancements or losses was found for untreated, heated and filtered samples  
195 (see Figs S1-S4). This indicates that most of the changes in INPs observed may occur on shorter timescales than those studied  
196 here, i.e.  $< 24$  hours.

197 Figure 2 shows the ratio of stored sample to fresh sample INP concentrations for untreated precipitation samples stored under  
198 four conditions: **(a)** room temperature (21 – 23 °C), **(b)** refrigerated (+ 4 °C), **(c)** frozen (-20 °C) and **(d)** flash frozen with  
199 liquid nitrogen before storing at -20 °C. Markers above the 1:1 line indicate enhancements in INP concentration from the fresh

sample, while markers below indicate losses. For each temperature interval containing data from at least two sets of replicate samples, the average difference in stored:fresh concentration ratios between replicates are represented with grey bars to indicate measurement variability. Replicate samples were processed for each storage protocol so that impacts of sample handling can be distinguished from storage impacts. For example, if settling occurs in bulk rain samples that are then divided into smaller volumes prior to storage, INP concentrations may differ between replicates of the bulk sample. Thus, it is assumed that INP concentration changes that are greater than differences between replicates (grey bars in Figs 2-4) can be attributed to storage impacts. We also assume that stored:fresh INP concentration ratios of 1:1 indicate insensitivity to storage, although it is possible that enhancements and losses of equal magnitude could also result in a 1:1 concentration ratio.

Finally, Fisher's Exact Test was applied to frozen and unfrozen well fractions between each stored sample and its corresponding fresh sample at each of the 2 °C temperature intervals. Stored sample frozen well fractions that were significantly different ( $p < 0.01$ ) from fresh sample frozen well fractions are indicated with filled markers. The term "significant" henceforth is intended to describe INP losses or enhancements that correspond to frozen well fractions that are determined to be significantly different from corresponding fresh sample frozen well fractions, according to Fisher's Exact Test (i.e. filled markers in Figs. 2-4). Results in Fig. 2 show that significant enhancements or losses of INPs occurred in all storage protocols between -9 and -17 °C, and that on average, stored samples exhibit INP losses (as indicated by the mean change in each temperature interval). In frozen and flash frozen samples, all enhancements and losses fall within  $\pm 1$  order of magnitude, whereas several significant INP losses beyond 1 order of magnitude are shown in room and refrigerated samples. INP concentration changes  $\geq 1$  order of magnitude are greater than changes in the ratios of the total insoluble particle population 10 – 2000 nm during storage (see Fig. S6). This indicates that the INPs in these samples are more sensitive to storage than the total insoluble particle population. Fig. S5 illustrates the impacts of the 4 storage protocols on the full IN spectra of a select untreated precipitation sample at two time intervals, 27 days and 64 days after collection.

Figure 3 shows the effects of storage on INP observations in heat-treated precipitation samples. Non-heat-labile INPs represented the majority (62% on average at -15 °C, see Sec. 3.1) of the total INPs observed in the fresh samples (i.e. 38% of the INPs in fresh samples were heat-labile). Fewer significant losses of non-heat-labile INPs are observed for heat-treated samples stored at room temperature and at 4 °C compared with untreated samples. Again, slightly fewer (2-3) of the total frozen and flash frozen samples exhibit significant losses and enhancements. All observations other than the one significantly enhanced sample in (b) fall within ranges of stored:fresh ratios observed in the total insoluble particle population (see Fig. S7, within an order of magnitude). This demonstrates that non-heat-labile INPs are generally less sensitive to storage than the total INP population (Fig. 2).

Effects of storage protocol on INP concentrations of filtered precipitation samples are shown in Figure 4 (0.45  $\mu\text{m}$  syringe filter, see Sect. 2.2 for details). INPs  $> 0.45\mu\text{m}$  represented the majority (52 and 63 % on average at -11 and -15 °C, respectively, see Sec. 3.1) of total INPs measured in the fresh precipitation samples. A higher number of filter-treated samples exhibit significant losses across all 4 storage types when compared with the untreated samples. Furthermore,

233 significant losses > 1 order of magnitude are observed across all storage types indicating that INPs < 0.45  $\mu\text{m}$  are generally  
234 more sensitive to storage than the total INP population present in precipitation samples.

235 As the stored:fresh ratios follow a log-normal distribution (one-sample Kolmogorov-Smirnov test), the uncertainties  
236 associated with storage and 95% confidence intervals were calculated in using the geometric mean and standard deviation of  
237 ratios of unique samples only between -9 and -17  $^{\circ}\text{C}$  (i.e. omitting any replicates, see Tables 5-7). . .

238

#### 239 **4. Discussion**

240 The challenge in selecting a storage protocol for atmospheric samples (e.g. precipitation, cloud water, ambient atmosphere) is  
241 that the INP population composition is unknown, diverse, and the impact of any given technique on the different species may  
242 vary. Many types of aerosols can serve as INPs, including dusts, metals and metal oxides, organic and glassy aerosols,  
243 bioaerosols, organic and mineral soil dust, and combustion products (Kanji et al., 2017). The aim of this study was to identify  
244 a storage protocol that best preserves the concentrations and characteristics of the general INP population observed in  
245 precipitation samples collected in a coastal environment. To this end, the impacts of 4 storage protocols on 15 untreated,  
246 heated, and filtered precipitation samples collected between September 22, 2015 and November 22, 2019 in La Jolla, CA were  
247 investigated by comparing measured INP concentrations between fresh and stored replicates. The fractions of INPs > 0.45  $\mu\text{m}$   
248 observed in this study varied between 52 and 63% at -11 and -15  $^{\circ}\text{C}$ , respectively. Excluding the five heat-treated samples  
249 in which INP concentrations were enhanced (e.g. 1.9 - 13X between -9 and -11  $^{\circ}\text{C}$ ), the average fraction of non-heat-labile  
250 INPs varied between 40 and 62% at -11 and -15  $^{\circ}\text{C}$ , respectively. INP enhancements in heat-treated samples are unexpected,  
251 as heat-treatments are typically applied assuming that heat destroys proteinaceous (e.g. biological) INPs. The causes of INP  
252 enhancements in heat-treated samples are unknown and have only been reported in coastal precipitation samples (Martin et  
253 al., 2017) and nascent sea spray aerosol (McCluskey et al., 2018). Possible sources include the redistribution of dissolved IN-  
254 active molecules onto particles (McCluskey et al. 2018), and the release of IN-active content from cells (McCluskey et al.  
255 2018, Wilson et al. 2015). These findings demonstrate that in samples influenced by marine sources, a superposition of both  
256 positive and negative  $\Delta\text{INP}$  in samples could result in the observed changes in INP concentrations post heat-treatment.

257 Additionally, the INP freezing temperatures and concentrations observed in this study compare with INPs observed in studies  
258 of marine and coastal environments (Fig. 1). As spectra in this regime (-5 to -20  $^{\circ}\text{C}$  and  $10^{-5}$  to  $\sim 10^{-1}$  per L air, respectively)  
259 cluster distinctly by source type (see Fig. 1-10 in Kanji et al., 2017), Fig. 1 indicates that the dominant sources to air masses  
260 sampled in this study were marine. Considering that data in this study compare well with marine and coastal INPs from a  
261 variety of marine-influenced air masses (DeMott et al., 2016, Yang et al., 2019), the findings herein are likely relevant to  
262 samples from other marine and coastal environments.

263 While mean INP changes are within a factor of ~2 or less of fresh sample INP concentrations for all protocols except “Room  
264 temperature” (Table 5), none of the 4 storage protocols prevented significant losses or enhancements of INP concentrations in  
265 all samples (Fig. 2), indicating that INP concentration measurements on fresh precipitation are superior to measurements on  
266 stored samples. 95% confidence intervals in Table 5 span losses > 1 order of magnitude in all protocols across multiple

267 temperature intervals. These uncertainties equal or exceed INP measurement uncertainties (1-2 orders of magnitude) at  
268 temperatures  $> -20$  °C due to discrepancies between instruments (DeMott et al., 2017). If correspondence within 1 order of  
269 magnitude (or 2-3 °C) is desired, uncertainties associated with storage should also be considered in studies using samples from  
270 coastal or marine environments. Thus, uncertainty distributions provided in Tables 5-7 can be used to evaluate observed INP  
271 concentrations and responses to treatments in the context of potential changes due to storage. However, the degree to which  
272 INP sensitivity to storage varies by INP source (e.g. with soil-derived INP populations) remains to be tested.

273 Samples stored under freezing and flash freezing conditions exhibited fewer changes overall compared to refrigerated samples.  
274 For example, at the INP activation temperature of -13 °C, in the rain sample that exhibited the highest sensitivity to storage,  
275 over 20% of the original concentration was preserved in the frozen sample, whereas only 5% of the original concentration was  
276 preserved in the refrigerated sample. These losses are more extreme than those of (Stopelli et al., 2014b), which demonstrated  
277 that INP concentrations of a snow sample refrigerated over 30 days decreased only two-fold from 0.027 to 0.013 L<sup>-1</sup> at -10 °C.  
278 Despite the range of enhancements and losses of heat-sensitive INPs observed in fresh samples, non-heat-labile INPs were  
279 generally less sensitive to storage than the total INP population, and with the exception of samples stored at room temperature,  
280 all techniques yielded similar results with fewer enhancements or losses. Interestingly, INPs  $< 0.45$  µm exhibited more  
281 sensitivity to all storage conditions tested than the total INP population, with significant losses (Fishers Exact Test,  $p < 0.01$ )  
282 observed in several samples leaving between 25% and 3% of the value observed in the original fresh sample. Losses of INPs  
283  $< 0.45$  µm in samples stored at room temperature and +4 °C were comparable to the losses of total INPs in untreated samples  
284 and are likely a result of chemical aging in solution. However, losses of INPs  $< 0.45$  micron in samples stored at -20 °C (both  
285 frozen and flash frozen) exceeded losses observed in the corresponding untreated samples. This is surprising given that a large  
286 fraction of INPs in this study were resilient to heat treatments of +95 °C. Lacking the identities of INPs observed in this study,  
287 a clear mechanism for their losses remains elusive. However, we offer the following points for consideration. It is well known  
288 that as a solution freezes, some solute is incorporated into the crystal and some is rejected, leading to enrichment of the solution  
289 phase and aggregation of dissolved or colloidal organic matter (Butler, 2002). Thus, as precipitation samples are freezing,  
290 small organic INPs may be lost simply due to aggregation in channels of enriched solute. In coastal precipitation samples for  
291 example, INPs may be so “lost” as the increased salinity in solution-phase channels destabilizes small suspended particles,  
292 allowing them to coagulate and settle (Jackson and Burd, 1998). Another possibility is that as the solution phase is enriched  
293 during freezing, smaller INPs may be adsorbing onto the surface of larger particles. The size distributions of total insoluble  
294 particles in the frozen samples show that most samples exhibit losses between 0-500 nm after storage and enhancements in  
295 sizes  $> 500$  nm (see Fig. S6). This effect is not observed for samples stored at room temperature or at +4 °C.

296 Changes in the total insoluble particle size distribution ( $\pm 1$  order of magnitude between 10 and 2000 nm, see Figs S6 and S7)  
297 may also have contributed to the observed INP concentration enhancements. Potential mechanisms for INP enhancements  
298 include increases in the number concentration of small particles due to breakup of loosely clumped masses of smaller particles,  
299 the redistribution of dissolved IN-active molecules onto particles (McCluskey et al. 2018), and the release of IN-active content  
300 from cells (McCluskey et al. 2018, Wilson et al. 2015) during cell death and lysis post freezing (Mazur et al., 1984).

301 Previous studies on precipitation collected along the California coast have demonstrated the contribution of dust, marine and  
302 terrestrial bioparticles to INPs in precipitation (Levin et al., 2019; Martin et al., 2019). Considering that well-characterized  
303 IN-active dust and biological standards (Arizona Test Dust and Snomax®, respectively) are sensitive to storage conditions, it  
304 is possible that dust or biological INPs contributed to the observed INP changes. Perkins et al. (2020) found that the IN-ability  
305 of Arizona Test Dust is degraded in most conditions, including aging in deionized water for 1 day, and results from Polen et  
306 al. (2016) show that the most efficient (i.e. warmest freezing) components of biological ice nucleators are also the most labile  
307 and sensitive to storage.

308 The observed distributions of INP concentration changes in stored precipitation samples have implications for the  
309 interpretation of heat and filtration treatment experiments. As heat denatures proteins, heat treatments are commonly used to  
310 infer contributions of proteinaceous or cellular contributions to INP populations, and filters are commonly applied to identify  
311 observed INP size ranges (e.g. McCluskey et al., 2018). For example, a typical analysis involves a comparison of the INP  
312 spectrum of an untreated sample to that of the heat-treated or filtered sample, and information about the sizes and biological  
313 composition of INPs are derived from this comparison. Our results demonstrate that these treatments may yield different  
314 results if treatments are applied to stored samples. Any losses of INPs due to filtering or heat application could be confounded  
315 by significant enhancements or losses caused by storage (up to > 1 order of magnitude), resulting in inaccurate conclusions  
316 about INP characteristics. In this study, a large fraction (30% to 48%, on average) of INPs observed in fresh precipitation  
317 samples were < 0.45  $\mu\text{m}$ . Considering this and that INPs < 0.45  $\mu\text{m}$  exhibit significant losses across all storage types, there is  
318 a risk that filter-treatments on stored samples in this study would lead to the underestimation of INPs < 0.45  $\mu\text{m}$ . Losses of  
319 heat-labile INPs in storage could also impact treatment outcomes on stored samples. Assuming negligible effects of storage  
320 on the heat-treated sample but losses due to storage in the untreated sample (e.g. as was shown to be most likely for untreated  
321 samples stored at +4  $^{\circ}\text{C}$ ), INP spectra of heat-treated samples could appear to indicate the entire INP population was heat-  
322 insensitive. This effect was observed in several samples across storage types (see Fig. S8).

## 323 5. Conclusions

324 Based on all observations in this study, we provide the following recommendations for precipitation samples collected in  
325 coastal and marine environments for offline INP analyses:

- 327 1. Of the 4 storage protocols tested, none prevented changes in INP concentrations across all samples between -7 and -  
328 19  $^{\circ}\text{C}$ . However, whenever processing fresh samples is not possible, our results demonstrate that storage at -20  $^{\circ}\text{C}$   
329 causes the least changes in INP concentrations.
- 330 2. Estimates of uncertainty attributed to storage impacts and 95% confidence intervals for INP measurements obtained  
331 from stored samples are provided (see Tables 5-7).
- 332 3. Flash freezing with liquid nitrogen before storing at -20  $^{\circ}\text{C}$  did not improve conservation of INPs.
- 333 4. With the exception of warm-freezing INPs (freezing temperatures  $\geq -9$   $^{\circ}\text{C}$ ) in samples stored at room temperature,  
334 we found little to no correlation between changes in INP concentrations and storage intervals on timescales between

335 1-166 days, indicating that most enhancements or losses are likely happening during freezing or on timescales < 24  
336 hours.

337 5. INPs that are insensitive to heat treatments are also less sensitive to storage. However, potential enhancements or  
338 losses due to storage (e.g. an average loss of 50% for INPs with freezing temperatures  $\geq -15^{\circ}\text{C}$  in samples stored at  
339  $-20^{\circ}\text{C}$ ) should be treated as additional uncertainty in measurements of INP concentration when comparing heat-  
340 treated with untreated INP spectra.

341 6. Due to the significant losses of INPs  $< 0.45 \mu\text{m}$  in storage, regardless of protocol, we recommend applying filtration  
342 treatments to fresh samples exclusively.

343 As measurements of INPs suspended in precipitation samples are used to infer in-cloud INP composition and  
344 concentration estimates, they represent important contributions to studies of links between aerosols, cloud processes and  
345 precipitation outcomes. This study derives bounds and correction factors for the impacts of storage on INPs and treatment  
346 outcomes from changes in INPs observed in coastal precipitation samples. However, it remains to be seen how INP  
347 sensitivity to storage varies by environment or INP composition. Further studies are needed to bracket storage effects on  
348 INP populations with various distributions of terrestrial and marine sources, as well as on heat-labile (biological) INPs,  
349 and INPs with colder activation temperatures. These studies could additionally benefit from analysis on how storage  
350 impacts differential INP spectra, which could reveal how sensitivity to storage varies by specific freezing temperature  
351 ranges. Bounds on the impact of storage will enable more meaningful intercomparisons of datasets and illuminate best  
352 practices for preserving INPs for offline analysis.

353  
354 *Data Availability:* The data set supporting this manuscript is hosted by the UCSD Library Digital Collections  
355 (<https://doi.org/10.6075/J0M32T8B>).

356  
357 *Supplement Link:* The supplement related to this article is available online at:

358  
359 *Author Contributions:* CMB wrote the manuscript, prepared figures, led the field campaign and laboratory analysis. DL  
360 contributed to the preparation of figures, precipitation sample collection and laboratory analysis. MDS, TCH, PJD and KAP  
361 provided feedback on the analyses and manuscript. KAP and PJD are principal investigators on awards CHE-1801971 and  
362 AGS-1451347.

363  
364 *Competing Interests:* The authors declare no competing interests.

365  
366 *Acknowledgements:* This work was supported by NSF through the NSF Center for Aerosol Impacts on Chemistry of the  
367 Environment (CAICE) CHE- 1801971 and AGS-1451347The National Weather Service Weather Prediction Center provided

368 the surface analysis satellite composite products used in this study. The AR data were provided by Bin Guan via  
369 <https://ucla.box.com/ARcatalog>. Development of the AR detection algorithm and databases was supported by NASA.  
370  
371

372 **References**

373 Agresti, A. and Coull, B. A.: Approximate Is Better than “Exact” for Interval Estimation of Binomial Proportions, *Am. Stat.*,  
374 52(2), 119–126, doi:10.2307/2685469, 1998.

375 Beall, C. M., Stokes, M. D., Hill, T. C., DeMott, P. J., DeWald, J. T., and Prather, K. A.: Automation and heat transfer  
376 characterization of immersion mode spectroscopy for analysis of ice nucleating particles, *Atmos. Meas. Tech.*, 10, 2613–2626,  
377 doi:10.5194/amt-10-2613-2017, 2017.

378 Budke, C. and Koop, T.: BINARY: An optical freezing array for assessing temperature and time dependence of heterogeneous  
379 ice nucleation, *Atmos. Meas. Tech.*, 8(2), 689–703, doi:10.5194/amt-8-689-2015, 2015.

380 Butler, M. F.: Freeze Concentration of Solutes at the Ice/Solution Interface Studied by Optical Interferometry, *Cryst. Growth  
381 Des.*, 2(6), 541–548, doi:10.1021/cg025591e, 2002.

382 Christner, B. C., Cai, R., Morris, C. E., McCarter, K. S., Foreman, C. M., Skidmore, M. L., Montross, S. N. and Sands, D. C.:  
383 Geographic, seasonal, and precipitation chemistry influence on the abundance and activity of biological ice nucleators in rain  
384 and snow., *Proc. Natl. Acad. Sci. U. S. A.*, 105(48), 18854–18859, doi:10.1073/pnas.0809816105, 2008a.

385 Christner, B. C., Morris, C. E., Foreman, C. M., Cai, R. and Sands, D. C.: Ubiquity of Biological Ice Nucleators in Snowfall,  
386 *Science* (80), 319(5867), 1214 LP – 1214, doi:10.1126/science.1149757, 2008b.

387 Conen, F., Eckhardt, S., Gundersen, H., Stohl, A. and Yttri, K. E.: Rainfall drives atmospheric ice-nucleating particles in the  
388 coastal climate of southern Norway, (2013), 11065–11073, 2017.

389 Creamean, J. M., Suski, K. J., Rosenfeld, D., Cazorla, A., DeMott, P. J., Sullivan, R. C., White, A. B., Ralph, F. M., Minnis,  
390 P., Comstock, J. M., Tomlinson, J. M. and Prather, K. A.: Dust and biological aerosols from the Sahara and Asia influence  
391 precipitation in the Western U.S, *Science* (80- ), 340(6127), 1572–1578, doi:10.1126/science.1227279, 2013.

392 Creamean, J. M., Mignani, C., Bukowiecki, N. and Conen, F.: Using freezing spectra characteristics to identify ice-nucleating  
393 particle populations during the winter in the Alps, *Atmos. Chem. Phys.*, 19(12), 8123–8140, doi:10.5194/acp-19-8123-2019,  
394 2019.

395 DeMott, P. J., Prenni, a J., Liu, X., Kreidenweis, S. M., Petters, M. D., Twohy, C. H., Richardson, M. S., Eidhammer, T. and  
396 Rogers, D. C.: Predicting global atmospheric ice nuclei distributions and their impacts on climate., *Proc. Natl. Acad. Sci. U.  
397 S. A.*, 107(25), 11217–22, doi:10.1073/pnas.0910818107, 2010.

398 DeMott, P. J., Hill, T. C. J., Petters, M. D., Bertram, A. K., Tobo, Y., Mason, R. H., Suski, K. J., McCluskey, C. S., Levin, E.  
399 J. T., Schill, G. P., Boose, Y., Rauker, A. M., Miller, A. J., Zaragoza, J., Rocci, K., Rothfuss, N. E., Taylor, H. P., Hader, J.

400 D., Chou, C., Huffman, J. A., Pöschl, U., Prenni, A. J. and Kreidenweis, S. M.: Comparative measurements of ambient  
401 atmospheric concentrations of ice nucleating particles using multiple immersion freezing methods and a continuous flow  
402 diffusion chamber, *Atmos. Chem. Phys.*, 17(18), 11227–11245, doi:10.5194/acp-17-11227-2017, 2017.

403 Failor, K. C., Iii, D. G. S., Vinatzer, B. A. and Monteil, C. L.: Ice nucleation active bacteria in precipitation are genetically  
404 diverse and nucleate ice by employing different mechanisms, , 1–14, doi:10.1038/ismej.2017.124, 2017.

405 Fleming, P. J. and Wallace, J. J.: How Not to Lie with Statistics: The Correct Way to Summarize Benchmark Results, *Commun.*  
406 *ACM*, 29(3), 218–221, doi:10.1145/5666.5673, 1986.

407 Guan, B. and Waliser, D. E.: Detection of atmospheric rivers: Evaluation and application of an algorithm for global studies, *J.*  
408 *Geophys. Res. Atmos.*, 120(24), 12514–12535, doi:doi:10.1002/2015JD024257, 2015.

409 Guan, B., Waliser, D. E. and Ralph, F. M.: An Intercomparison between Reanalysis and Dropsonde Observations of the Total  
410 Water Vapor Transport in Individual Atmospheric Rivers, *J. Hydrometeorol.*, 19(2), 321–337, doi:10.1175/JHM-D-17-0114.1,  
411 2018.

412 Hader, J. D., Wright, T. P. and Petters, M. D.: Contribution of pollen to atmospheric ice nuclei concentrations, *Atmos. Chem.*  
413 *Phys.*, 14(11), 5433–5449, doi:10.5194/acp-14-5433-2014, 2014.

414 Harrison, A. D., Whale, T. F., Rutledge, R., Lamb, S., Tarn, M. D., Porter, G. C. E., Adams, M. P., McQuaid, J. B., Morris,  
415 G. J. and Murray, B. J.: An instrument for quantifying heterogeneous ice nucleation in multiwell plates using infrared emissions  
416 to detect freezing, *Atmos. Meas. Tech.*, 11(10), 5629–5641, doi:10.5194/amt-11-5629-2018, 2018.

417 Hegg, D. A. and Hobbs, P. V: Measurements of sulfate production in natural clouds, *Atmos. Environ.*, 16(11), 2663–2668,  
418 doi:10.1016/0004-6981(82)90348-1, 1982.

419 Hill, T. C. J., Moffett, B. F., DeMott, P. J., Georgakopoulos, D. G., Stump, W. L. and Franc, G. D.: Measurement of ice  
420 nucleation-active bacteria on plants and in precipitation by quantitative PCR, *Appl. Environ. Microbiol.*, 80(4), 1256–1267,  
421 doi:10.1128/AEM.02967-13, 2014.

422 Hill, T. C. J., DeMott, P. J., Tobo, Y., Fröhlich-Nowoisky, J., Moffett, B. F., Franc, G. D. and Kreidenweis, S. M.: Sources of  
423 organic ice nucleating particles in soils, *Atmos. Chem. Phys. Discuss.*, (January), 1–37, doi:10.5194/acp-2016-1, 2016.

424 Hoose, C., Kristjánsson, J. E., Chen, J.-P. and Hazra, A.: A Classical-Theory-Based Parameterization of Heterogeneous Ice  
425 Nucleation by Mineral Dust, Soot, and Biological Particles in a Global Climate Model, *J. Atmos. Sci.*, 67(8), 2483–2503,  
426 doi:10.1175/2010JAS3425.1, 2010.

427 Huffman, J. A., Prenni, A. J., Demott, P. J., Pöhlker, C., Mason, R. H., Robinson, N. H., Fröhlich-Nowoisky, J., Tobo, Y.,  
428 Després, V. R., Garcia, E., Gochis, D. J., Harris, E., Müller-Germann, I., Ruzene, C., Schmer, B., Sinha, B., Day, D. A.,  
429 Andreae, M. O., Jimenez, J. L., Gallagher, M., Kreidenweis, S. M., Bertram, A. K. and Pöschl, U.: High concentrations of  
430 biological aerosol particles and ice nuclei during and after rain, *Atmos. Chem. Phys.*, 13(13), 6151–6164, doi:10.5194/acp-13-  
431 6151-2013, 2013.

432 Jackson, G. A. and Burd, A. B.: Aggregation in the Marine Environment, *Environ. Sci. Technol.*, 32(19), 2805–2814,  
433 doi:10.1021/es980251w, 1998.

434 Joyce, R. E., Lavender, H., Farrar, J., Werth, J. T., Weber, C. F., D'Andrilli, J., Vaitilingom, M. and Christner, B. C.: Biological  
435 Ice-Nucleating Particles Deposited Year-Round in Subtropical Precipitation, edited by A. J. M. Stams, *Appl. Environ.*  
436 *Microbiol.*, 85(23), e01567-19, doi:10.1128/AEM.01567-19, 2019.

437 Kanji, Z. A., Ladino, L. A., Wex, H., Boose, Y., Burkert-Kohn, M., Cziczo, D. J. and Krämer, M.: Overview of Ice Nucleating  
438 Particles, *Meteorol. Monogr.*, 58, 1.1-1.33, doi:10.1175/AMSMONOGRAPH-D-16-0006.1, 2017.

439 Kulmala, M., Laaksonen, A., J.Charlson, R. and Korhonen, P.: Clouds without supersaturation, *Nature*, 388(6640), 336–337,  
440 doi:10.1038/41000, 1997.

441 Ladino, L. A., Yakobi-Hancock, J. D., Kilthau, W. P., Mason, R. H., Si, M., Li, J., Miller, L. A., Schiller, C. L., Huffman, J.  
442 A., Aller, J. Y., Knopf, D. A., Bertram, A. K. and Abbatt, J. P. D.: Addressing the ice nucleating abilities of marine aerosol: A  
443 combination of deposition mode laboratory and field measurements, *Atmos. Environ.*, 132, 1–10,  
444 doi:10.1016/j.atmosenv.2016.02.028, 2016.

445 Lim, Y. B., Tan, Y., Perri, M. J., Seitzinger, S. P. and Turpin, B. J.: Aqueous chemistry and its role in secondary organic  
446 aerosol (SOA) formation, *Atmos. Chem. Phys.*, 10(21), 10521–10539, doi:10.5194/acp-10-10521-2010, 2010.

447 Lohmann, U.: A glaciation indirect aerosol effect caused by soot aerosols, *Geophys. Res. Lett.*, 29(4), 11–14,  
448 doi:10.1029/2001GL014357, 2002.

449 Lohmann, U. and Feichter, J.: Global indirect aerosol effects: a review, *Atmos. Chem. Phys.*, 5(3), 715–737, doi:10.5194/acp-  
450 5-715-2005, 2005.

451 Martin, A. C., Cornwell, G., Beall, C. M., Cannon, F., Reilly, S., Schaap, B., Lucero, D., Creamean, J., Ralph, F. M., Mix, H.  
452 T. and Prather, K.: Contrasting local and long-range-transported warm ice-nucleating particles during an atmospheric river in  
453 coastal California, USA, *Atmos. Chem. Phys.*, 19(7), 4193–4210, doi:10.5194/acp-19-4193-2019, 2019.

454 Mason, R. H., Chou, C., McCluskey, C. S., Levin, E. J. T., Schiller, C. L., Hill, T. C. J., Huffman, J. a., DeMott, P. J. and  
455 Bertram, a. K.: The micro-orifice uniform deposit impactor–droplet freezing technique (MOUDI-DFT) for measuring  
456 concentrations of ice nucleating particles as a function of size: improvements and initial validation, *Atmos. Meas. Tech.*, 8(6),  
457 2449–2462, doi:10.5194/amt-8-2449-2015, 2015.

458 Mazur, P.: Freezing of living cells: mechanisms and implications, *Am. J. Physiol. Physiol.*, 247(3), C125–C142,  
459 doi:10.1152/ajpcell.1984.247.3.C125, 1984.

460 McCluskey, C. S., Hill, T. C. J., Sultana, C. M., Laskina, O., Trueblood, J., Santander, M. V, Beall, C. M., Michaud, J. M.,  
461 Kreidenweis, S. M., Prather, K. A., Grassian, V. and DeMott, P. J.: A Mesocosm Double Feature: Insights into the Chemical  
462 Makeup of Marine Ice Nucleating Particles, *J. Atmos. Sci.*, 75(7), 2405–2423, doi:10.1175/JAS-D-17-0155.1, 2018.

463 McElfresh, C., Harrington, T. and Vecchio, K. S.: Application of a novel new multispectral nanoparticle tracking technique,  
464 *Meas. Sci. Technol.*, 29(6), 65002, doi:10.1088/1361-6501/aab940, 2018.

465 Michaud, A. B., Dore, J. E., Leslie, D., Lyons, W. B., Sands, D. C. and Priscu, J. C.: Biological ice nucleation initiates hailstone  
466 formation, *J. Geophys. Res. Atmos.*, 119(21), 12,112–186,197, doi:10.1002/2014JD022004, 2014.

467 Monteil, C. L., Bardin, M. and Morris, C. E.: Features of air masses associated with the deposition of *Pseudomonas syringae*

468 and *Botrytis cinerea* by rain and snowfall, , 8(11), 2290–2304, doi:10.1038/ismej.2014.55, 2014.

469 Morris, C. E., Sands, D. C., Vinatzer, B. A., Glaux, C., Guilbaud, C., Buffière, A., Yan, S., Dominguez, H. and Thompson, B.

470 M.: The life history of the plant pathogen *Pseudomonas syringae* is linked to the water cycle, *Isme J.*, 2, 321, 2008.

471 Morris, C. E., Conen, F., Alex Huffman, J., Phillips, V., Pöschl, U. and Sands, D. C.: Bioprecipitation: A feedback cycle

472 linking Earth history, ecosystem dynamics and land use through biological ice nucleators in the atmosphere, *Glob. Chang.*

473 *Biol.*, 20(2), 341–351, doi:10.1111/gcb.12447, 2014.

474 Perkins, R. J., Gillette, S. M., Hill, T. C. J. and DeMott, P. J.: The Labile Nature of Ice Nucleation by Arizona Test Dust, *ACS*

475 *Earth Sp. Chem.*, 4(1), 133–141, doi:10.1021/acsearthspacechem.9b00304, 2020.

476 Petters, M. D. and Wright, T. P.: Revisiting ice nucleation from precipitation samples, *Geophys. Res. Lett.*, 42(20), 8758–

477 8766, doi:doi:10.1002/2015GL065733, 2015.

478 Polen, M., Lawlis, E. and Sullivan, R. C.: The unstable ice nucleation properties of Snomax ® bacterial particles, ,

479 doi:10.1002/2016JD025251, 2016.

480 Prenni, A. J., Tobo, Y., Garcia, E., DeMott, P. J., Huffman, J. A., McCluskey, C. S., Kreidenweis, S. M., Prenni, J. E., Pöhlker,

481 C. and Pöschl, U.: The impact of rain on ice nuclei populations at a forested site in Colorado, *Geophys. Res. Lett.*, 40(1), 227–

482 231, doi:10.1029/2012GL053953, 2013.

483 Rangel-Alvarado, R. B., Nazarenko, Y. and Ariya, P. A.: Snow-borne nanosized particles: Abundance, distribution,

484 composition, and significance in ice nucleation processes, *J. Geophys. Res. Atmos.*, 120(22), 11,711–760,774,

485 doi:10.1002/2015JD023773, 2015.

486 Rogers, D. C., DeMott, P. J., Kreidenweis, S. M. and Chen, Y.: Measurements of ice nucleating aerosols during SUCCESS,

487 *Geophys. Res. Lett.*, 25(9), 1383, doi:10.1029/97GL03478, 1998.

488 Šantl-Temkiv, T., Sahyoun, M., Finster, K., Hartmann, S., Augustin-Bauditz, S., Stratmann, F., Wex, H., Clauss, T., Nielsen,

489 N. W., Sørensen, J. H., Korsholm, U. S., Wick, L. Y. and Karlson, U. G.: Characterization of airborne ice-nucleation-active

490 bacteria and bacterial fragments, *Atmos. Environ.*, 109, 105–117, doi:10.1016/j.atmosenv.2015.02.060, 2015.

491 Schnell, R. C.: Ice Nuclei in Seawater, Fog Water and Marine Air off the Coast of Nova Scotia: Summer 1975, *J. Atmos. Sci.*,

492 34(8), 1299–1305, doi:10.1175/1520-0469(1977)034<1299:INISFW>2.0.CO;2, 1977.

493 Smith, A. W., Skilling, D. E., Castello, J. D. and Rogers, S. O.: Ice as a reservoir for pathogenic human viruses: specifically,

494 caliciviruses, influenza viruses, and enteroviruses, *Med. Hypotheses*, 63(4), 560–566, doi:10.1016/j.mehy.2004.05.011, 2004.

495 Stopelli, E., Conen, F., Zimmermann, L., Alewell, C. and Morris, C. E.: Freezing nucleation apparatus puts new slant on study

496 of biological ice nucleators in precipitation, *Atmos. Meas. Tech.*, 7(1), 129–134, doi:10.5194/amt-7-129-2014, 2014.

497 Stopelli, E., Conen, F., Morris, C. E., Herrmann, E., Bukowiecki, N. and Alewell, C.: Ice nucleation active particles are

498 efficiently removed by precipitating clouds, *Sci. Rep.*, 5, 16433, doi:10.1038/srep16433, 2015.

499 Stopelli, E., Conen, F., Guilbaud, C., Zopfi, J., Alewell, C. and Morris, C. E.: Ice nucleators, bacterial cells and *Pseudomonas*

500 *syringae* in precipitation at Jungfraujoch, *Biogeosciences*, 14(5), 1189–1196, doi:10.5194/bg-14-1189-2017, 2017.

501 Tan, I., Storelvmo, T. and Zelinka, M. D.: Observational constraints on mixed-phase clouds imply higher climate sensitivity,

502 Science (80), 352(6282), 224 LP – 227, doi:10.1126/science.aad5300, 2016.

503 Vali, G.: Freezing Nucleus Content of Hail and Rain in Alberta, J. Appl. Meteorol., 10(1), 73–78, 1971.

504 Vali, G.: Comments on “Freezing Nuclei Derived from Soil Particles,” J. Atmos. Sci., 31(5), 1457–1459, doi:10.1175/1520-  
505 0469(1974)031<1457:CONDTS>2.0.CO;2, 1974.

506 Vali, G.: Sizes of Atmospheric Ice Nuclei, Nature, 212(5060), 384–385, doi:10.1038/212384a0, 1966.

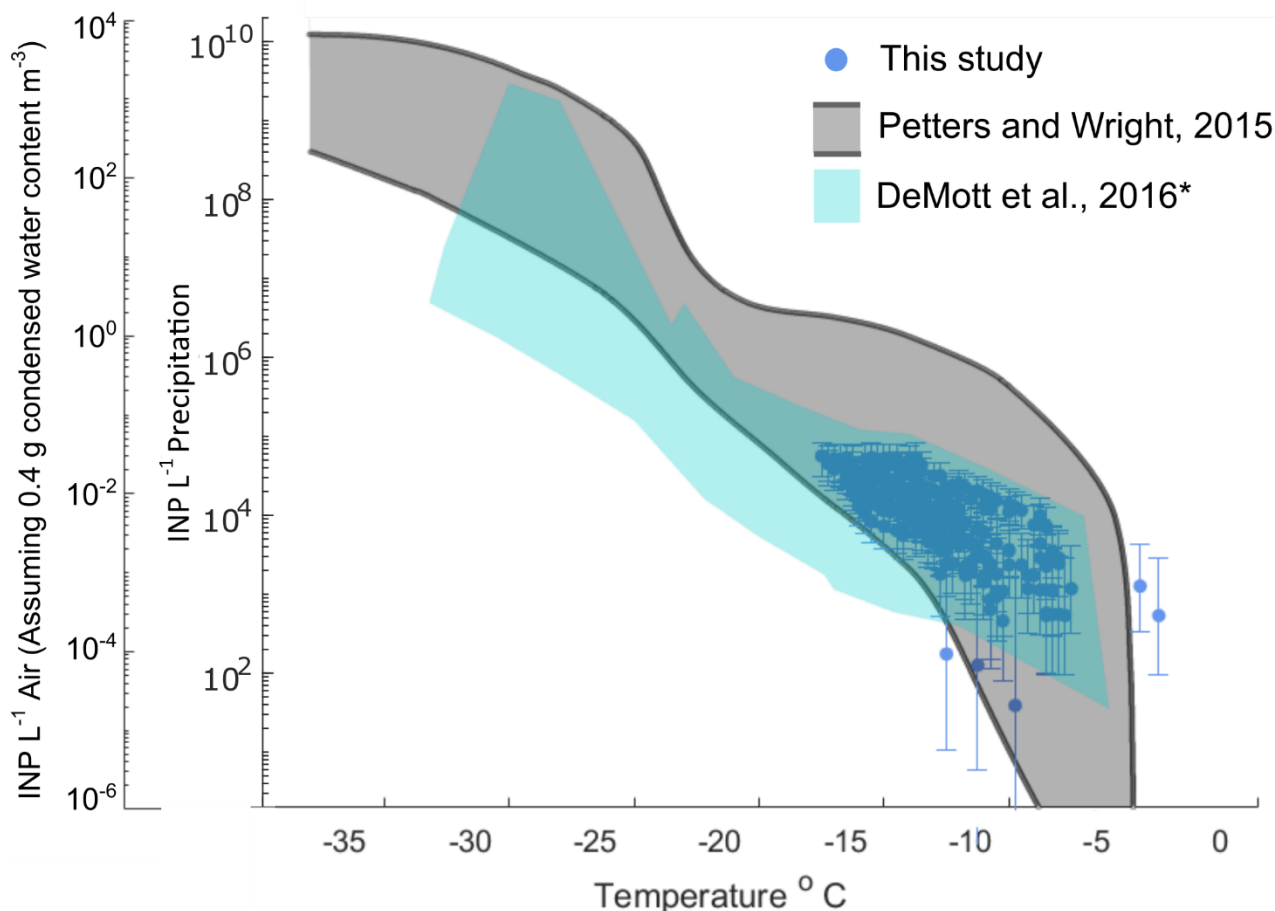
507 Vasebi, Y., Mechan Llontop, M. E., Hanlon, R., Schmale III, D. G., Schnell, R. and Vinatzer, B. A.: Comprehensive  
508 characterization of an aspen (*Populus tremuloides*) leaf litter sample that maintained ice nucleation activity for 48 years,  
509 Biogeosciences, 16(8), 1675–1683, doi:10.5194/bg-16-1675-2019, 2019.

510 Wex, H., Augustin-Bauditz, S., Boose, Y., Budke, C., Curtius, J., Diehl, K., Dreyer, A., Frank, F., Hartmann, S., Hiranuma,  
511 N., Jantsch, E., Kanji, Z. A., Kiselev, A., Koop, T., Möhler, O., Niedermeier, D., Nillius, B., Röschen, M., Rose, D., Schmidt,  
512 C., Steinke, I. and Stratmann, F.: Intercomparing different devices for the investigation of ice nucleating particles using  
513 Snomax® as test substance, Atmos. Chem. Phys., 15(3), 1463–1485, doi:10.5194/acp-15-1463-2015, 2015.

514 Wex, H., Huang, L., Zhang, W., Hung, H., Traversi, R., Becagli, S., Sheesley, R. J., Moffett, C. E., Barrett, T. E., Bossi, R.,  
515 Skov, H., Hünerbein, A., Lubitz, J., Löffler, M., Linke, O., Hartmann, M., Herenz, P. and Stratmann, F.: Annual variability of  
516 ice-nucleating particle concentrations at different Arctic locations, Atmos. Chem. Phys., 19(7), 5293–5311, doi:10.5194/acp-  
517 19-5293-2019, 2019.

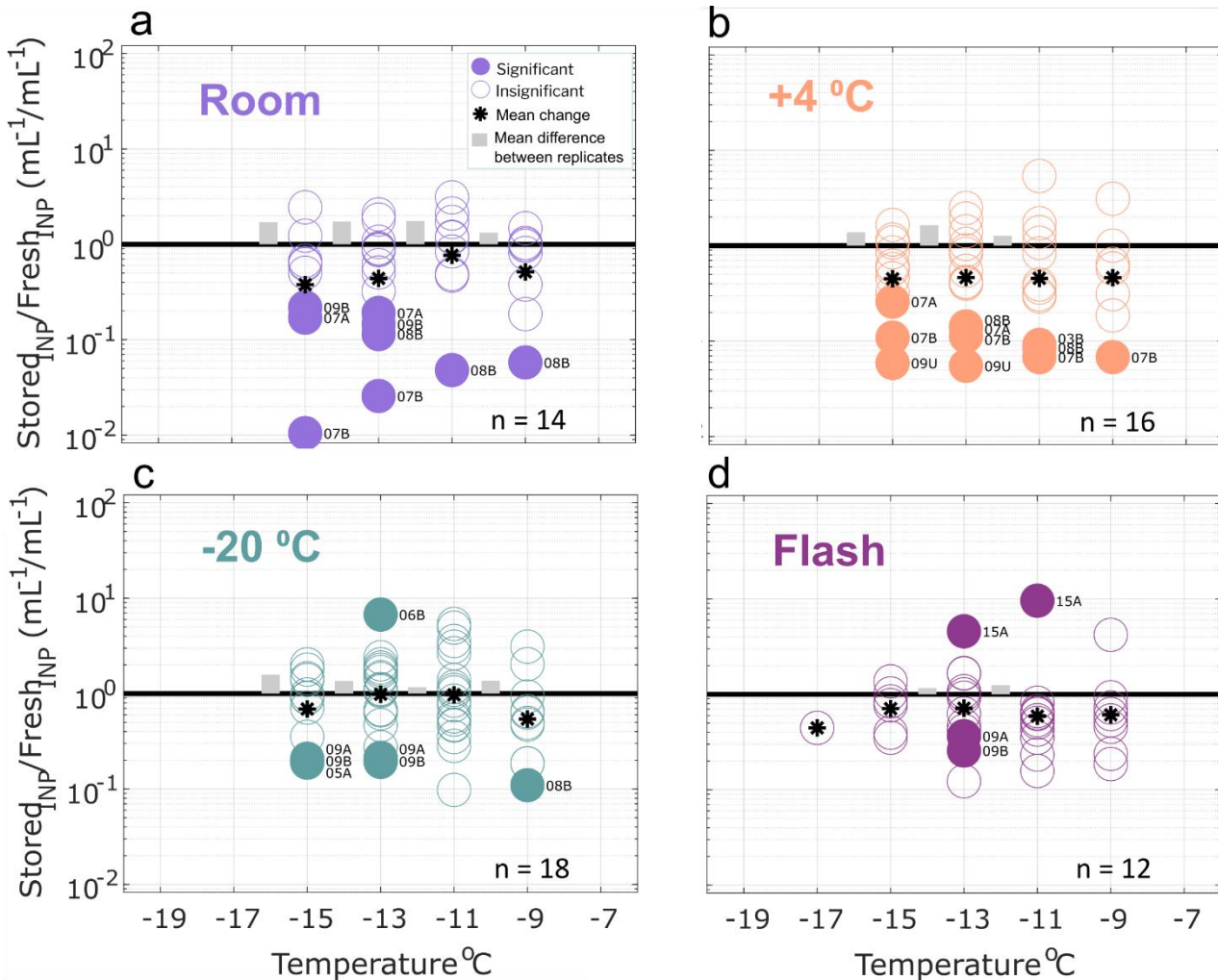
518 Whale, T. F., Murray, B. J., O’Sullivan, D., Wilson, T. W., Umo, N. S., Baustian, K. J., Atkinson, J. D., Workneh, D. A. and  
519 Morris, G. J.: A technique for quantifying heterogeneous ice nucleation in microlitre supercooled water droplets, Atmos. Meas.  
520 Tech., 8(6), 2437–2447, doi:10.5194/amt-8-2437-2015, 2015. Wright, T. P., Hader, J. D., McMeeking, G. R. and Petters, M.  
521 D.: High relative humidity as a trigger for widespread release of ice nuclei, Aerosol Sci. Technol., 48(11), i–v,  
522 doi:10.1080/02786826.2014.968244, 2014.

523 Yang, J., Wang, Z., Heymsfield, A. J., DeMott, P. J., Twohy, C. H., Suski, K. J. and Toohey, D. W.: High ice concentration  
524 observed in tropical maritime stratiform mixed-phase clouds with top temperatures warmer than  $-8^{\circ}\text{C}$ , Atmos. Res., 233,  
525 104719, doi:<https://doi.org/10.1016/j.atmosres.2019.104719>, 2020.

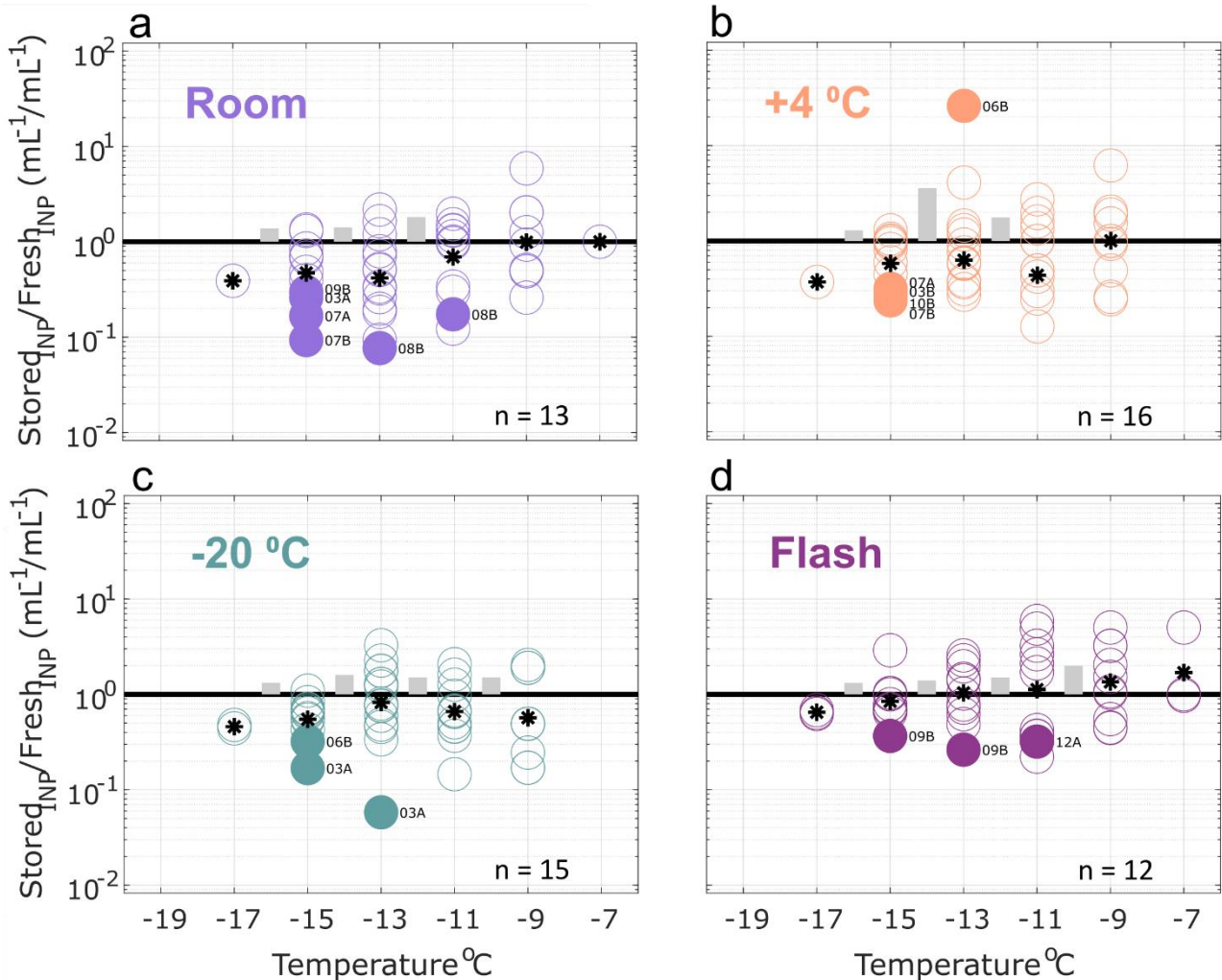


526  
527 **Figure 1: INP concentrations per liter of precipitation and estimated in-cloud INP concentrations per volume of air in**  
528 **15 precipitation samples collected at two coastal sites at Scripps Institution of Oceanography (La Jolla, California,**  
529 **USA) between 9/22/2016 and 11/22/2019.** Grey shaded region indicates the spectrum of INP concentrations reported in 9  
530 **previous studies of precipitation and cloud water samples collected from various seasons and locations worldwide, adapted**  
531 **from Fig. 1 in (Petters and Wright, 2015).** The blue shaded region denotes the composite spectrum of INP concentrations  
532 **observed in a range of marine and coastal environments including the Caribbean, East Pacific and Bering Sea as well as**  
533 **laboratory-generated nascent sea spray (DeMott et al., 2016).**

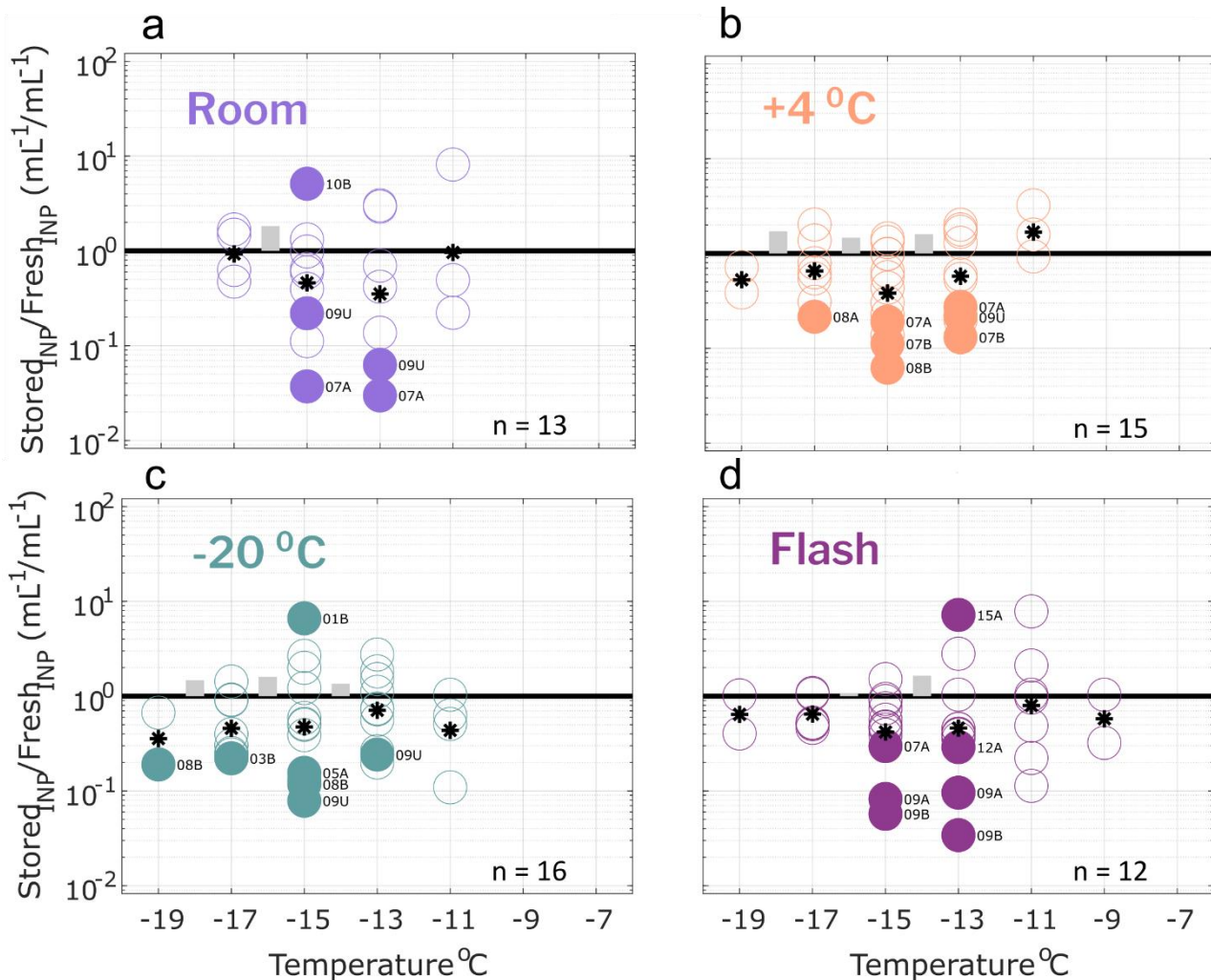
534 \*DeMott et al., 2016 data has been updated with a completed dataset for the ICE-T study, as shown in Yang et al., 2020



536  
537 **Figure 2: Ratio of INP concentrations measured in untreated precipitation samples (stored:fresh), calculated in**  
538 **successive 2  $^{\circ}\text{C}$  increments between -19 and -7  $^{\circ}\text{C}$ .** Four storage protocols were applied: (a) room temperature (21-23  $^{\circ}\text{C}$ ),  
539 (b) refrigerated (+4  $^{\circ}\text{C}$ ), (c) frozen (-20  $^{\circ}\text{C}$ ) and (d) flash freezing in liquid nitrogen before storing frozen (-20  $^{\circ}\text{C}$ ). All samples  
540 were processed at one or two time intervals between 1 and 166 days post-collection (see Figs S1-S4). For samples processed  
541 at two intervals, both replicate samples are represented in the figure for a total of 14, 16, 18 and 12 samples in (a), (b), (c) and  
542 (d), respectively (see Table 2 for summary of sample and replicate numbers). Markers above black 1:1 line indicate  
543 enhancement of INP concentrations in stored samples, and markers below indicate losses. In temperature intervals containing  
544 stored:fresh ratios from at least two sets of replicate samples, grey bars represent the average difference between replicates.  
545 Stored sample frozen well fractions that passed Fishers Exact Test ( $p < 0.01$ ) for significant differences from original fresh  
546 sample frozen well fractions at each of the 5 temperatures are indicated with filled markers, and the mean change in each  
547 temperature interval is marked with a star. Significant data are also labelled to indicate the sample number (01-15, see Table  
548 1), and replicate ("A" or "B", and "U" indicates there were no replicates for the sample). Results show that on average, INP  
549 concentrations decrease in stored samples, and that both room temperature storage and refrigeration result in significant  
550 INP losses. Frozen and flash frozen storage show comparable results, with fewer (3-4) of the observations exhibiting significant  
551 losses and enhancements in INP concentrations.



556 **Figure 3: Ratio of INP concentrations measured in heated precipitation samples (stored:fresh), calculated in successive**  
 557 **2 °C increments between -19 and -7 °C.** Same samples as shown in Figure 2, but heated to 95 °C for 20 minutes prior to  
 558 measurement to eliminate heat-labile INPs (see Methods Sect. 2.2 for details). All samples were processed at one or two time  
 559 intervals between 1 and 166 days post-collection. For samples processed at two intervals, both replicate samples are  
 560 represented in the figure for a total of 13, 16, 15 and 12 samples in (a), (b), (c) and (d), respectively (see Table 3 for summary  
 561 of sample and replicate numbers). In temperature intervals containing stored:fresh ratios from at least two sets of replicate  
 562 samples, grey bars represent the average difference between replicates. Results show significant losses of INPs in heat-treated  
 563 samples stored at room temperature. Refrigerated, frozen, and flash frozen samples show comparable results with a few (1-3)  
 564 samples exhibiting significant losses and enhancements. Non-heat-labile INPs are generally less sensitive to storage protocol  
 565 than the total INP population in precipitation samples (Fig. 2), with the exception of storage at room temperature.



566  
567 **Figure 4: Ratio of INP concentrations measured in filtered (0.45  $\mu\text{m}$ ) precipitation samples (stored:fresh), calculated**  
568 **in successive 2  $^{\circ}\text{C}$  increments between -19 and -7  $^{\circ}\text{C}$ . Same samples as in Fig. 2 but filtered with a 0.45  $\mu\text{m}$  syringe filter**  
569 **prior to measurement (see Methods Sect. 2.2 for details). All samples were processed at one or two time intervals between 1**  
570 **and 166 days post-collection. For samples processed at two intervals, both replicate samples are represented in the figure for**  
571 **a total of 13, 15, 16 and 12 samples in (a), (b), (c) and (d), respectively (see Table 4 for summary of sample and replicate**  
572 **numbers). In temperature intervals containing stored:fresh ratios from at least two sets of replicate samples, grey bars represent**  
573 **the average difference between replicates. Results show significant losses of INPs in several filtered samples, regardless of**  
574 **storage protocol.**

**Table 1. Precipitation sampling periods**

| Sampling Period | UTC Date   | UTC time start | UTC time end     | Meteorological Conditions                               |
|-----------------|------------|----------------|------------------|---|
| 1               | 9/22/2016  | 19:20          | 21:13            | scattered, low coastal clouds, lack of dynamical system |
| 2               | 9/22/2016  | 19:42          | 21:13            | scattered, low coastal clouds, lack of dynamical system |
| 3               | 12/31/2016 | 4:53           | 7:52             | warm, low cloud rain                                    |
| 4               | 1/1/2017   | 7:53           | 10:52            | post-frontal rain, meso-scale system                    |
| 5               | 1/5/2017   | 21:02          | 22:01            | pre-frontal rain, meso-scale system                     |
| 6               | 1/9/2017   | 15:51          | 19:50            | decaying atmospheric river                              |
| 7               | 1/11/2017  | 19:00          | 23:30            | frontal rain  |
| 8               | 1/14/2017  | 2:03           | 6:00             | warm, low cloud rain                                    |
| 9               | 1/19/2017  | 12:30          | 17:30            | pre-frontal rain, meso-scale system                     |
| 10              | 1/20/2017  | 14:15          | 02:20 (next day) | weak atmospheric river                                  |
| 11              | 11/19/2019 | 22:34          | 22:45            | pre-frontal rain, meso-scale system                     |
| 12              | 11/22/2019 | 4:43           | 5:42             | scattered, low coastal clouds, lack of dynamical system |
| 13              | 11/22/2019 | 6:43           | 7:42             | scattered, low coastal clouds, lack of dynamical system |
| 14              | 11/23/2019 | 7:42           | 8:41             | convective, local updraft rain                          |
| 15              | 11/23/2019 | 8:42           | 9:41             | convective, local updraft rain                          |

575

576

577

578

579

580

581

582

583

584

585

586

587

588

**Table 2. Summary of unique and replicate untreated precipitation samples used for INP concentration measurements featured in Fig. 2.**

| Storage technique             | No. of unique samples | No. of stored samples measured at 2 timesteps |
|-------------------------------|-----------------------|---|
| Room temperature (19 - 23 °C) | 8                     | 6   |
| Refrigeration (+4 °C)         | 8                     | 8   |
| Freezing (-20 °C)             | 9                     | 9   |
| Flash freezing (-20 °C)       | 8                     | 4   |

**Table 3. Summary of unique and replicate heat-treated precipitation samples used for INP concentration measurements featured in Fig. 3.**

| Storage technique             | No. of unique samples | No. of stored samples measured at 2 timesteps |
|-------------------------------|-----------------------|---|
| Room temperature (19 - 23 °C) | 8                     | 6   |
| Refrigeration (+4 °C)         | 8                     | 8   |
| Freezing (-20 °C)             | 8                     | 7   |
| Flash freezing (-20 °C)       | 8                     | 4   |

**Table 4. Summary of unique and replicate filtered (0.45 µm) precipitation samples used for INP concentration measurements featured in Fig. 4.**

| Storage technique             | No. of unique samples | No. of stored samples measured at 2 timesteps |
|-------------------------------|-----------------------|---|
| Room temperature (19 - 23 °C) | 8                     | 5   |
| Refrigeration (+4 °C)         | 8                     | 7   |
| Freezing (-20 °C)             | 9                     | 7   |
| Flash freezing (-20 °C)       | 8                     | 4   |

**Table 5. Estimate of uncertainty associated with storage impacts for INPs with activation temperatures between -9 and -17 °C measured in stored, untreated precipitation samples.** Confidence intervals were derived from the log-normal distribution of changes observed in INP concentrations due to storage (see Fig. 2 and details in Sect. 3.2). Temperature intervals where datapoints were too few to derive confidence intervals are indicated with “NA”. Changes in INP concentration corresponding to enhancements or losses greater than 1 order of magnitude (losses <= -90% or enhancements >= +900%) in bold.

| Storage protocol               | Mean Change<br>-9 °C<br>(%) | 95% CI<br>Low<br>(%) | 95% CI<br>High<br>(%) | Mean Change<br>-11 °C<br>(%) | 95% CI<br>Low<br>(%) | 95% CI<br>High<br>(%) | Mean Change<br>-13 °C<br>(%) | 95% CI<br>Low<br>(%) | 95% CI<br>High<br>(%) | Mean Change<br>-15 °C<br>(%) | 95% CI<br>Low<br>(%) | 95% CI<br>High<br>(%) |
|--------------------------------|-----------------------------|----------------------|-----------------------|------------------------------|----------------------|-----------------------|------------------------------|----------------------|-----------------------|------------------------------|----------------------|-----------------------|
| Room temperature (21 - 23 °C)* | -26                         | -82                  | +200                  | -51                          | <b>-97</b>           | +850                  | -77                          | <b>-98</b>           | +220                  | -77                          | <b>-99</b>           | <b>+1000</b>          |
| Refrigeration (+4 °C)*         | -42                         | -74                  | +32                   | -74                          | <b>-99</b>           | +400                  | -46                          | <b>-95</b>           | +520                  | -56                          | <b>-95</b>           | +290                  |
| Freezing (-20 °C)              | -48                         | <b>-95</b>           | +430                  | -16                          | <b>-90</b>           | +580                  | +24                          | -80                  | +650                  | -50                          | <b>-90</b>           | +150                  |
| Flash freezing (-20 °C)        | -21                         | <b>-90</b>           | +520                  | -41                          | <b>-95</b>           | +560                  | -33                          | <b>-91</b>           | +390                  | NA                           | NA                   | NA                    |

\* For INPs with freezing temperatures >= -9 °C, changes in INP concentrations are moderately correlated with time in samples stored at room temperature or at +4 °C (see Sec. 3.2). Change factors for room temperature and refrigerated storage protocols are derived from samples stored in ranges of 27 – 76 and 8 – 46 days, respectively.

**Table 6. Estimate of uncertainty associated with storage impacts for INPs with activation temperatures between -9 and -17 °C measured in stored, heat-treated precipitation samples.**

Confidence intervals were derived from the log-normal distribution of changes observed in INP concentrations due to storage (see Fig. 3 and details in Sect. 3.2). Changes in INP concentration corresponding to enhancements or losses greater than 1 order of magnitude (losses <= -90% or enhancements >= +900%) in bold.

| Storage protocol              | Mean   | 95%        | 95%         | Mean   | 95%        | Mean         | 95%    | 95%        | Mean         | 95%    | 95%        |          |
|-------------------------------|--------|------------|-------------|--------|------------|--------------|--------|------------|--------------|--------|------------|----------|
|                               | Change | CI         | CI          | Change | CI         |              | 95% CI | Change     | CI           | 95% CI | Change     | CI       |
|                               | -9 °C  | Low        | High        | -11 °C | Low        | High (%)     | -13 °C | Low        | High (%)     | -15 °C | Low        | High (%) |
| Room temperature (21 - 23 °C) | +32    | -74        | +550        | -17    | -86        | +380         | -65    | <b>-95</b> | +155         | -58    | <b>-93</b> | +150     |
| Refrigeration (+4 °C)         | -56    | <b>-91</b> | <b>+940</b> | -74    | <b>-99</b> | <b>+1600</b> | -58    | <b>-99</b> | <b>+6000</b> | -60    | -87        | +27      |
| Freezing (-20 °C)             | -55    | <b>-91</b> | +130        | -53    | -87        | +69          | -42    | <b>-93</b> | +390         | -34    | -70        | +47      |
| Flash freezing (-20 °C)       | +36    | -76        | +660        | +31    | -88        | <b>+1300</b> | -9.0   | -81        | +340         | +1.0   | -60        | +150     |

**Table 7. Estimate of uncertainty associated with storage impacts for INPs with activation temperatures between -11 and -19 °C measured in stored, filtered precipitation samples.** Confidence intervals were derived from the log-normal distribution of changes observed in INP concentrations due to storage (see Fig. 2 and details in Sect. 3.2). Temperature intervals where datapoints were too few to derive confidence intervals are indicated with “NA”. Changes in INP concentration corresponding to enhancements or losses greater than 1 order of magnitude (losses <= -90% or enhancements >= +900%) in bold.

| Storage protocol              | Mean Change<br>-11 °C<br>(%) | 95% CI<br>Low (%) | 95% CI<br>High (%) | Mean Change<br>-13 °C<br>(%) | 95% CI<br>Low (%) | 95% CI<br>High (%) | Mean Change<br>-15 °C<br>(%) | 95% CI<br>Low (%) | 95% CI<br>High (%) | Mean Change<br>-17 °C<br>(%) | 95% CI<br>Low (%) | 95% CI<br>High (%) |
|-------------------------------|------------------------------|-------------------|--------------------|------------------------------|-------------------|--------------------|------------------------------|-------------------|--------------------|------------------------------|-------------------|--------------------|
| Room temperature (21 - 23 °C) | NA                           | NA                | NA                 | -80                          | <b>-99</b>        | +360               | -72                          | <b>-96</b>        | +130               | -7.0                         | -68               | +170               |
| Refrigeration (+4 °C)         | NA                           | NA                | NA                 | -48                          | <b>-94</b>        | +300               | -65                          | <b>-97</b>        | +250               | -14                          | -80               | +250               |
| Freezing (-20 °C)             | NA                           | NA                | NA                 | -31                          | -89               | +330               | -54                          | <b>-98</b>        | +870               | -32                          | -78               | +110               |
| Flash freezing (-20 °C)       | -26                          | -83               | +230               | -65                          | <b>-98</b>        | +650               | -68                          | <b>-96</b>        | +140               | NA                           | NA                | NA                 |